Monograph:

Li, L.M. and Billings, S.A. (2005) A Volterra Modelling Study of the Duffing Oscillator. Research Report. ACSE Research Report 896 . Department of Automatic Control and Systems Engineering

A Volterra Modelling Study of the Duffing Oscillator

L.M.Li and S.A.Billings

Department of Automatic Control
and Systems Engineering,
University of Sheffield, Sheffield
Post Box 600 S1 3JD
UK

Research Report No. 896

May 2005

A Volterra Modelling Study of the Duffing Oscillator

L.M.Li and S.A.Billings*

Department of Automatic Control and Systems Engineering

University of Sheffield

Sheffield S1 3JD

UK

*S.Billings@sheffield.ac.uk

Abstract: Hysteresis is a common and severe nonlinear phenomenon associated with the Duffing oscillators, which can be induced by either varying the amplitude or the frequency of excitation. In this paper both cases are studied using the Volterra time and frequency domain modelling techniques.

1. Introduction

Oscillations widely exist in the physical world, especially in mechanical, electronic and marine systems. Although most systems are nonlinear to some extent, where possible, linearised models should be used because of the simplicity of analysis and availability of a relatively complete theory. However under certain conditions many physical systems are not even nearly linear, and new phenomena such as subharmonics, superharmonics, limit cycles, and chaos can be observed. Important theoretical results on these topics can be found in the books of Stoker(1950), Nayfeh and Mook(1979) and Hagedorn(1982), etc.

Duffing oscillators have been used to represent many practical systems and have often been used as benchmark examples for nonlinear oscillator analysis. The present study focuses on an important nonlinear phenomenon, the jump phenomenon, of the Duffing oscillator. Jump phenomena can occur when either the amplitude or the frequency of the excitation is varied and both types of jump phenomena are investigated in this study. First, the validity of the Volterra series representation for the Duffing-Ueda oscillator excited by a single-tone excitation within a low excitation amplitude range, where the system has multiple-valued response solutions, is assessed, and an additional model is derived to accommodate the Volterra representation for different ranges. These analyses are then extended to represent the jump phenomenon of a typical Duffing oscillator when the frequency of the excitation increases while the amplitude of the excitation is held constant.

MO117790SH

2. Volterra Modelling in the Time and Frequency Domain

Volterra(1930) series modelling has been widely studied for the representation, analysis and design of nonlinear systems. The Volterra model is a direct generalisation of the linear convolution integral, therefore providing an intuitive representation in a simple and easy to apply way. For a SISO nonlinear system, with $u(t)$ and $y(t)$ the input and output respectively, the Volterra series can be expressed as

$$y(t) = \sum_{n=1}^{\infty} y_n(t) \qquad (1.a)$$

and $y_n(t)$ is the 'n-th order output' of the system

$$y_n(t) = \int_{-\infty}^{\infty} \cdots \int_{-\infty}^{\infty} h_n(\tau_1,\cdots,\tau_n) \prod_{i=1}^{n} u(t-\tau_i)d\tau_i \qquad n>0 \qquad (1.b)$$

where $h_n(\tau_1,\cdots,\tau_n)$ is called the 'nth-order kernel' or 'nth-order impulse response function'. If $n=1$, this reduces to the familiar linear convolution integral.
The discrete time domain counterpart of the continuous time domain SISO Volterra expression (1) is

$$y(k) = \sum_{n=1}^{\infty} y_n(k) \qquad (2.a)$$

where

$$y_n(k) = \sum_{-\infty}^{\infty} \cdots \sum_{-\infty}^{\infty} h_n(\tau_1,\cdots,\tau_n) \prod_{i=1}^{n} u(k-\tau_i) \qquad n>0, k \in Z \qquad (2.b)$$

In practice only the first few kernels are studied on the assumption that the contribution of the higher order kernels falls off rapidly. Systems that can be adequately represented by a Volterra series with just a few terms are called a weakly or mildly nonlinear system. A discrete time Volterra series is also called a NX (Nonlinear model with eXogenous inputs) model.

The multi-dimensional Fourier transform of $h_n(\cdot)$ yields the 'nth-order frequency response function' or the Generalised Frequency Response Function (GFRF):

$$H_n(\omega_1,\cdots,\omega_n) = \int_{-\infty}^{\infty} \cdots \int_{-\infty}^{\infty} h_n(\tau_1,\cdots,\tau_n) \exp(-j(\omega_1\tau_1 + \cdots + \omega_n\tau_n)) d\tau_1 \cdots d\tau_n \qquad (3)$$

The generalised frequency response functions represent an inherent and invariant property of the underlying system, and have proved to be an important analysis and design tool for characterising nonlinear phenomena. In practice, the GFRF's can be estimated using non-parametric or parametric methods. The parametric method involves mapping a nonlinear differential equation(Billings and Peyton Jones, 1990) or mapping a nonlinear difference equation(Peyton Jones and Billings, 1989) into the frequency domain using the probing method.

3. **Volterra Modelling for the Duffing-Ueda Equation with Varying Excitation Amplitude**

Considering the Duffing-Ueda oscillator

$$\frac{d^2y}{dt^2} + k\frac{dy}{dt} + \mu y^3 = E\cos(t) \quad (4)$$

Where μ is normally a small number. In this example, μ is chosen as 0.15, and k is chosen as 0.1.

By varying the external input amplitude E, the corresponding bifurcation diagram in Figure 1 can be produced. The Response Spectrum Map(RSM) introduced by Billings and Boaghe(2001), provids a frequency domain counterpart of the bifurcation diagram, and gives straightforward insight into the frequency domain behaviour of the system. The RSM for equation (4) is plotted in Figure 2.

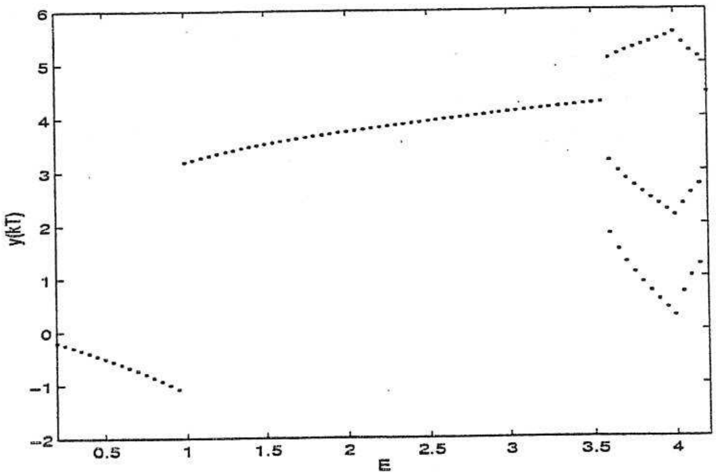

Figure 1. Bifurcation diagram for Duffing-Ueda equation (4)

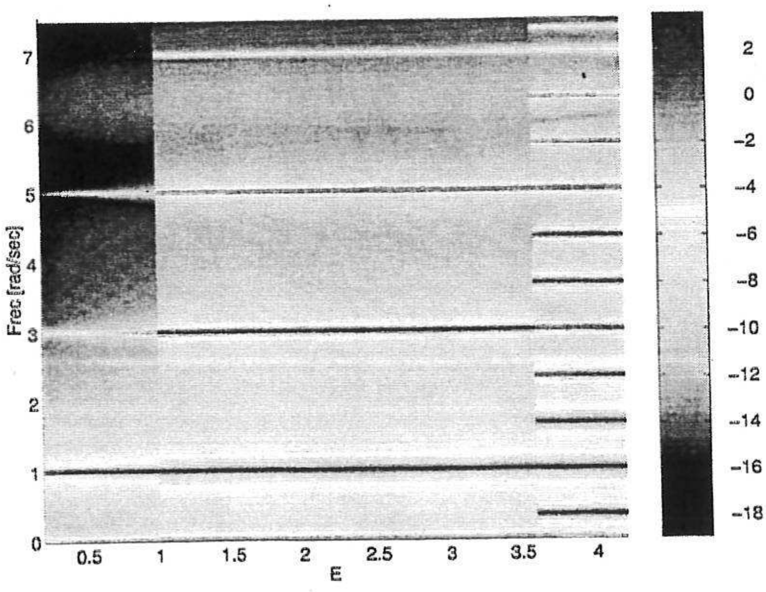

Figure 2. Response Spectrum Map(RSM) for Duffing-Ueda equation (4)

Figure 2 shows that for the initial amplitude variation in [0.2 3.5] the harmonic content consists of a dominant frequency component at the driving frequency of 1 rad/sec and odd multiples of the driving frequency at 3, 5, 7 rad/sec. As the amplitude E increases, a third order subharmonic occurs at around 3.5 rad/sec. It is well-known that generally Volterra series cannot represent subharmonic systems. Hence this study will focus on the Volterra modelling for $0 < E < 3.5$.

Inspection of both Figure 1 and 2 shows that although for both the input amplitude ranges $E \in [0.2\ 0.9]$ and $E \in (0.9\ 3.5]$ no subharmonics exist and the output response has the same period, the responses are significantly different in amplitude. This is usually called a jump phenomenon or hysteresis. The amplitudes of response for each value of E can be roughly estimated using the harmonic balance method as below. Because the linear damping factor k is not zero, there will be an intermediate phase angle shift with the response. Instead of writing $u = E\sin(t)$ for the excitation and $y = C\sin(t-\varphi)$ for the dominant periodic solution, it is more convenient to write

$$\begin{cases} u = P\sin(t) + Q\cos(t) \quad \text{with } E = \sqrt{P^2+Q^2}, \text{and} \\ \qquad\qquad y = C\sin(t) \end{cases} \tag{5}$$

Substituting (5) into (4), together with the use of $\sin^3(t) = \frac{3}{4}\sin(t) - \frac{1}{4}\sin(3t)$ yields

$$\tfrac{3}{4}\mu C^3\sin(t) - C\sin(t) + kC\cos(t) = P\sin(t) + Q\cos(t) \tag{6}$$

where the term containing $\sin(3t)$ has been neglected.

Equating coefficients of the same harmonic terms in (6) and using $E = \sqrt{P^2+Q^2}$ gives

$$(\tfrac{3}{4}\mu C^3 - C)^2 + k^2C^2 = E^2 \tag{7}$$

Equation (7) gives the approximate relationship between the amplitude of excitation and the amplitude of response.

For the specific values of the coefficients in equation (4), that is, $k = 0.1$ and $\mu = 0.15$, the multiple amplitude solutions for C can be obtained for each value of E. Following the actual amplitude shown in Figure 1, the middle solutions were neglected, leaving the two solution curves of (7) shown in Figure 3.

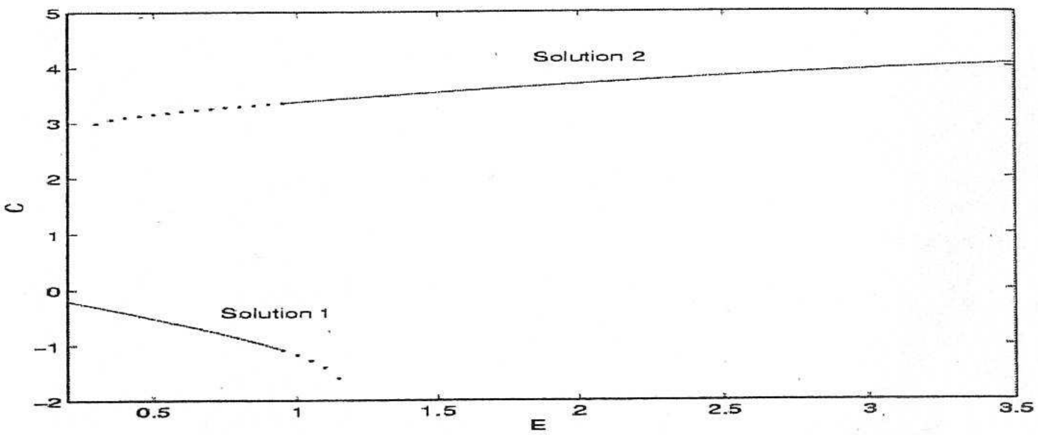

Figure 3. Response amplitude curves using the harmonic balance method

The solid line in Figure 3 is used to reflect the fact that the amplitude of the response jumps, making it comparable with the bifurcation diagram Figure 1. Figure 3 agrees well with Figure 1 for the excitation range [0.2 3.5].

Both the bifurcation diagram in Figure 1 and the Response Spectrum Map in Figure 2 clearly reveal the jump phenomenon around the point of excitation amplitude E=1. Moreover, the time invariant and analytical nature of the Duffing-Ueda equation (4) suggests that for the excitation variation range [0.2 3.5] the system is weakly nonlinear and can therefore be represented by a Volterra series. The Volterra series representation could be derived from the GFRF's obtained by mapping equation (4) into the frequency domain(Billings and Peyton Jones, 1990). However the GFRF's for any system representation result in a unique steady state solution. In the current example, the GFRF's from (4) will only provide an explanation for solution 1 trajectory, along the solid and dotted lines in Figure 3, but will fail to explain the response along solution 2 trajectory. Therefore an additional analysis is needed to find a Volterra representation for the solution 2 trajectory, and this is one of the main objectives of this study. To this end, the system (4) was simulated using a Fourth order Runge-Kutta algorithm for excitation amplitude E=1 at a sampling frequency $f_s = 120/\pi$ with zero initial conditions. By using the input-output data a simple discrete time NARX model was identified (Billings and Chen, 1998) as

$$y(k) = 1.99738\, y(k\text{-}1) - 0.99738\; y(k-2) - 0.00010260\, y^3(k-1) + 0.0006848\, u(k-2) \tag{8}$$

The GFRF's associated with this model were obtained by mapping (8) into the frequency domain(Billings and Peyton Jones, 1990). $H_1(\omega)$ for model (8), and for comparison, $H_1(\omega)$ from the continuous time model (4), are plotted in Figure 4. It can be seen that $H_1(\omega)$ from (8) is almost the same as $H_1(\omega)$ from (4), indicating that (8) is nothing more than the discrete time version of (4). Equation (8) will therefore produce the same bifurcation diagram and response spectrum map as (4) and will only be valid in the sense of the Volterra representation along 'solution 1' in Figure 3.

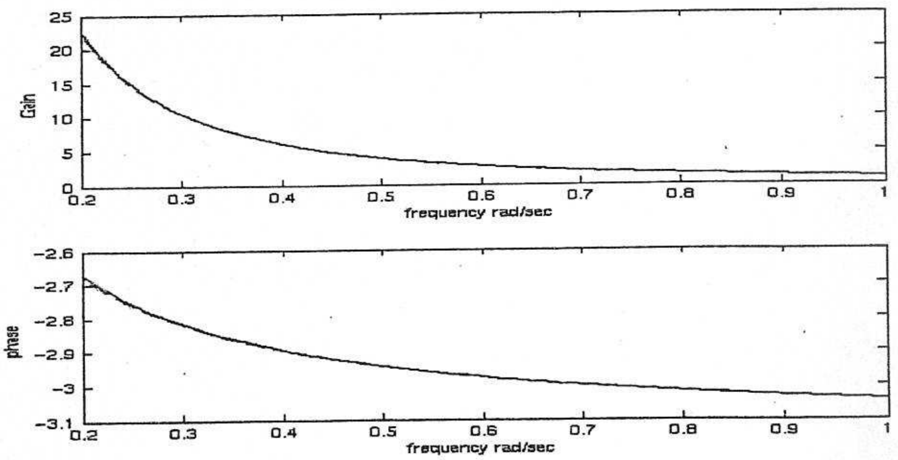

Figure 4. $H_1(\omega)$ **from (8)—solid, and** $H_1(\omega)$ **from (4) — dashed**

The same input-output data used in the identification of model (8) were then used in a different model structure—in either a NARX model, or a NX model form. This time a new identified discrete time model was obtained which is capable of providing a frequency domain solution along 'solution 2' trajectory in Figure 3. One such model is given below:

$$y(k) = 33.180\,u(k-2) - 30.466\,u(k-1) + 23.288u^3(k-2) + 22.754u(k-1)u^2(k-2) \tag{9}$$

This NX model is actually a truncated discrete time Volterra model of the form of equation (2).

The GFRF's can be derived directly from equation (9). Only the first and the third order GFRF's exist for equation (9) and these can be used to synthesis the response. Figure 5 shows both the first and up to third order nonlinear output responses. It can be seen that an excellent solution is achieved using the truncated third order Volterra series representation.

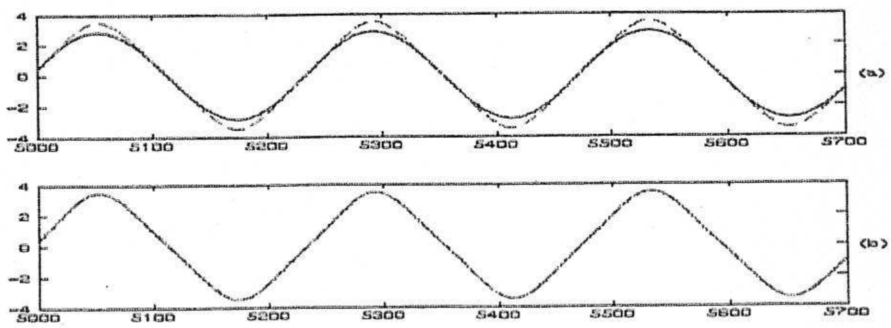

Figure 5 (a) First order output response, and (b) up to the third order response Solid— synthesized output from the GFRF's of eqn (9); Dashed-- original output from (4)

The decomposed output response for each frequency component can easily be obtained using the GFRF's. The fundamental frequency component(excitation frequency) comes from the first order and the third order GFRF's contributions, and the amplitude can be determined as $C_{-GFRF's} = 3.2717$, which is very close to the harmonic balance solution, $C_{-harmonic} = 3.3720$ at the excitation amplitude $E = 1$ in equation (8).

4. Volterra Modelling for the Duffing Equation with Varying Excitation Frequency

Hysteresis can also occur when the frequency of the excitation changes. Consider the following Duffing equation

$$\frac{d^2y}{dt^2} + 0.2\frac{dy}{dt} + y + 0.05y^3 = A\cos(\omega t) \tag{10}$$

with fixed excitation amplitude $A = 1$. The dynamics of (10) have been studied by Thompson and Stewart(2002) with varying driving frequency ω. Generally there will be two jump paths corresponding to slowly-increasing and slowly-decreasing ω. In this study, the time domain and frequency domain Volterra modelling for the increasing ω path will be investigated.

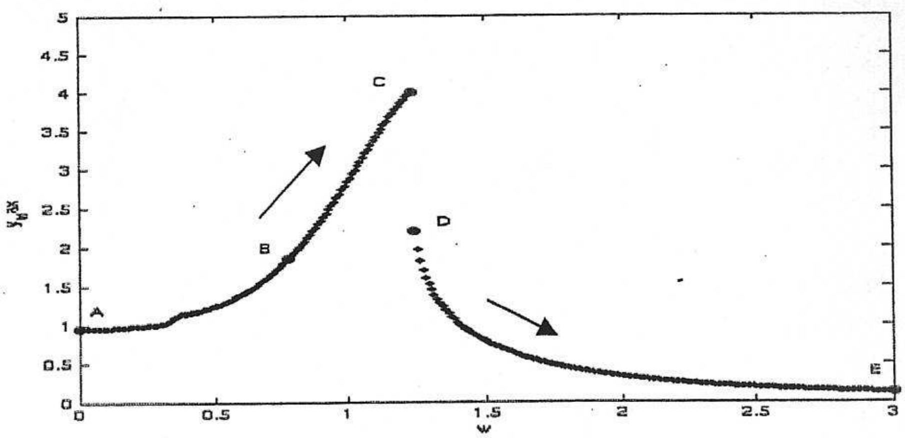

Figure 6. Resonance response curve for Duffing Equation (10)

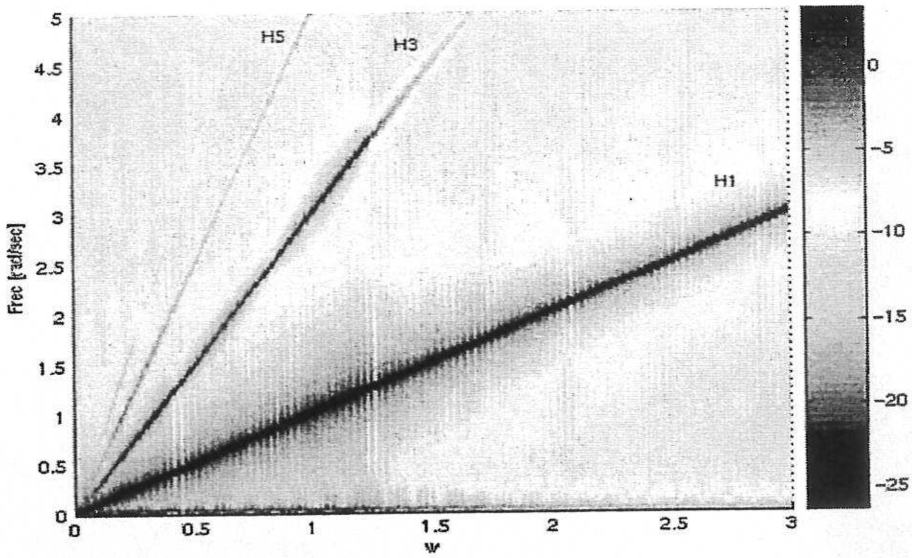

Figure 7. Response Spectrum Map for Duffing Equation (10)

The resonance response curve, which is the maximum amplitude of the response y versus the driving frequency ω, for Duffing equation (10) with increasing ω is shown in Figure 6. Clearly there is a jump in the response from point C to point D, which suggests a severe behaviour change at this location. This will be studied by an inspection of (10) in the frequency domain. This shows that as the frequency ω increases, the GFRF's derived from equation (10) are valid for the range A to B(ω=0.75rad/sec) in Figure 6. The GFRF's start to become invalid for the range B to C(ω=1.24) in Figure 6, and become valid again for the range D to E. In other words, in the frequency domain, besides the same jump point as in the time domain at ω=1.24, there is another change point at around ω=0.75. However, the change at around ω=0.75 develops gradually, and is not as abrupt as the 'jump' at ω=1.24. This kind of frequency domain change does not appear to be revealed by traditional tools, such as the resonance diagram in Figure 6. The Response Spectrum Map, which is plotted in Figure 7, does provide some information about this frequency domain change. First of all, there are no subharmonics shown in figure 7, suggesting that the system for the whole frequency range of interest is 'mildly' nonlinear and that a valid Volterra/frequency domain representation should exist over all the frequency range. Secondly, the apparent 'jump' from C to D at frequency point ω=1.24 in Figure 6 is not clearly detected by the first order(linear) harmonic line H1, but is clearly shown on the subsequent higher order harmonic lines H3, H5, etc by a stronger higher order harmonics presence. Finally the frequency domain change at point B in Figure 6 is not detected on the dominant first order(linear) harmonics line H1, but again the H3 line shows a significant third order harmonic change around the frequency point ω=0.75. In order to find the frequency domain representation for the range B to C, the technique in section 3 can be used repeatedly, that is, discrete time Volterra-- or equivalently NX—models can be identified from each pair of single tone excitation and response data, over the frequency range [0.75, 1.24]. For example, for excitation frequency $\omega=1$, the corresponding discrete time Volterra model can be expressed, with a sample frequency $f_s = 60/\pi$, as

$$y(k) = 26.816\,u(k-2) - 24.40\,u(k-1) + 1.3984\,u^3(k-2) - 1.3792\,u^2(k-1)u(k-2) \tag{11}$$

from which the $H_1(\cdot)$ and $H_3(\cdot)$ data at frequency $\omega=1$ can be obtained(Billings and Peyton Jones, 1990).

By repeating this procedure for a number of excitation frequencies along [0.75, 1.24], the GFRF's can be acquired by putting together the frequency response data recorded at each frequency point. The first order frequency response function $H_1(\cdot)$ computed in this manner is plotted in Figure 8 (dashed).

Using the approach introduced in Li and Billings(2001), a nonlinear continuous time model can be reconstructed from the $H_1(\cdot)$ and $H_3(\cdot)$ data, as been given below

$$y + 0.21727\tfrac{dy}{dt} + 0.87564\tfrac{d^2y}{dt^2} + 0.01713\tfrac{d^3y}{dt^3} + 0.18005\tfrac{d^4y}{dt^4} + 0.01939y^3 - 0.002162y^2\tfrac{dy}{dt}$$
$$-0.04358y(\tfrac{dy}{dt})^2 + 0.0001961(\tfrac{dy}{dt})^3 = 1.0037\cos(\omega t) \tag{12}$$

The $H_1(\cdot)$ computed from equation (12) (solid) is compared with the $H_1(\cdot)$ from the Volterra modelling such as equation (11), in Figure 8, which shows a good match.

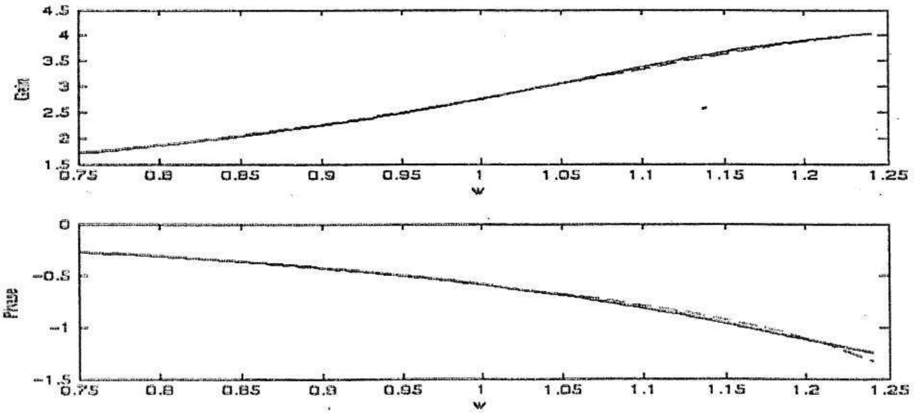

Figure 8. $H_1(\cdot)$ by reconstructed continuous time model (12) –solid and $H_1(\cdot)$ by Volterra modellings—dashed

To test the validity of the reconstructed continuous time model (12), arbitrarily choose an excitation frequency from the specific frequency range [0.75, 1.24], say, ω=0.9 rad/sec, and compare the response from the original Duffing equation (10) and the response synthesized from the GFRF's obtained from equation (12). It can be seen that up to third order GFRF's from (12) can provide a satisfactory representation for the system, as shown in Figure 9.

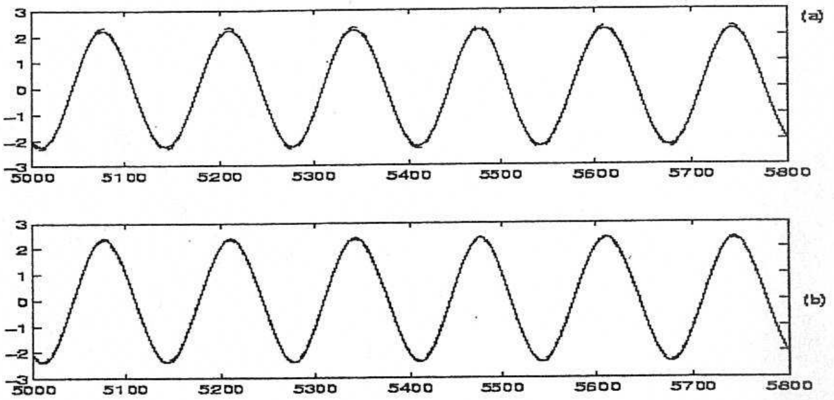

Figure 9 (a) First order output response, and (b) up to the third order response Solid— synthesized output by GFRF's from (12); Dashed--simulated original output from (10)

It is interesting to show the synthesised response result for the same frequency ω=0.9 rad/sec computed using the GFRF's from the original Duffing equation (10) as a comparison, in Figure 10. It can be seen that in this case the GFRF's from the original Duffing equation totally fail at this frequency.

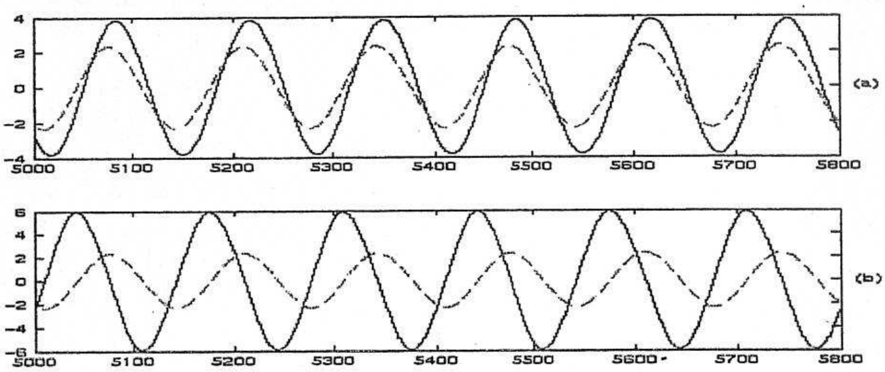

Figure 10 (a) First order output response, and (b) up to the third order response Solid— synthesized output by GFRF's from (10); Dashed--simulated original output from (10)

Therefore the whole picture of the frequency domain representation for the Duffing oscillator (10) when the excitation amplitude is fixed as A= 1 would look like Figure 11 for the first order frequency response function for example. This diagram is similar to the resonance response curve in Figure 6, but with one more 'jump' point at ω=0.75. In summary, the frequency response function initially follows H_1 from the original Duffing equation (10) from A to B, then jumps to H_1 by the new equation (12) from B to C, and finally jumps back to H_1 by the original Duffing equation (10) from D to E.

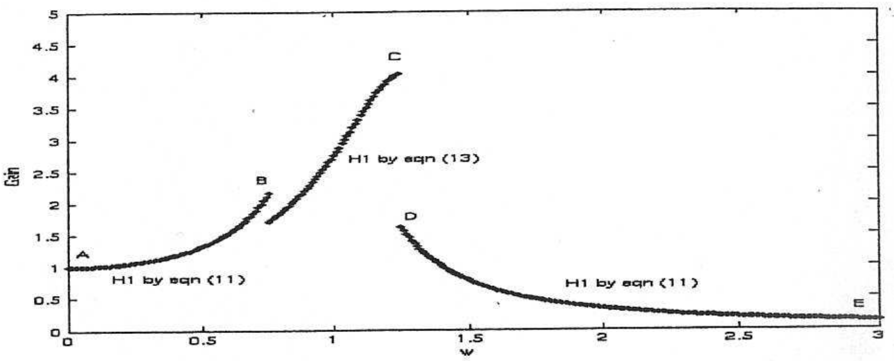

Figure 11. First order frequency domain response function for the Duffing oscillator (10)

5. Conclusions

Despite the apparent simplicity the Duffing oscillator can produce very complicated behaviours from weakly nonlinear leading quickly to chaos as the amplitude or frequency of the excitation is varied. Even over a low excitation range, the behaviour of this oscillator is not consistent and can exhibit jump phenomena, that is, the output response will jump from one trajectory to another.

It has been shown that the original Duffing-Ueda model is only valid in the Volterra/frequency domain sense for a very limited excitation range. For the majority of the excitation range, the original Duffing-Ueda equation losses the ability to provide a Volterra representation or frequency domain interpretation. In this paper it has been shown that additional models valid in the Volterra representation sense can be derived based on discrete time parametric modelling over different ranges. The original equation and the additional models and the frequency domain equivalents, GFRF's, form important new tools in the time and frequency domain analysis and design of the Duffing-Ueda oscillator.

It was also demonstrated that under certain circumstances the Duffing oscillator can lose some frequency domain properties as the frequency varies. It has been shown in this study that a new parametric modelling approach can provide the frequency features to fill in these gaps. This should help to better understand the behaviour of the Duffing oscillator.

Acknowledgement: The authors gratefully acknowledge that this work was supported by the Engineering and Physical Sciences Research Council(EPSRC) UK.

References:

Billings, S.A. and Boaghe, O.M., 2001,The response spectrum map, a frequency domain equivalent to the bifurcation diagram, Int. J. of Bifurcation and Chaos, Vol.11, No.7, pp.1961-1975.

Billings, S.A. and Chen, S., 1998, The determination of multivariable nonlinear models for dynamic systems using neural networks, Invited Chapter in 'Neural Network System Techniques and Applications' in the series 'Control and Dynamic Systems Vol 7', edited by C T Leondes, pp.231-278.

Billings, S.A. and Peyton Jones, J.C., 1990, Mapping non-linear integro-differential equations into the frequency domain, Int.J.Control, Vol. 52, No. 4,pp.863-879.
Hagedorn, P., 1982, *Non-linear oscillations*, Clarendon Press, Oxford.
Li, L.M. and Billings, S.A., 2001, Continuous time non-linear system identification in the frequency domain, Int J Control, 74 (10), pp. 1052-1061.
Nayfeh, A.H. and Mook, D.T., 1979, *Nonlinear oscillations*, John Wiley & Sons, New York,.
Peyton Jones, J.C. and Billings, S.A., 1989, A Recursive algorithm for computing the frequency response of a class of non-linear difference equation models, Int.J.Control, Vol.50, No.5, pp.1925-1940.
Stoker, J.J., 1950, *Nonlinear vibrations in Mechanical and Electrical Systems*, Interscience Publishers Inc, New York.
Thompson, J. M. T. and Stewart, H. B., 2002, Nonlinear Dynamics and Chaos, John Wiley & Sons Ltd, England.
Volterra, V., 1930, *Theory of Functionals*, Blackie and Sons.